The Temperature and Moisture Profile of Material by Drying during the Falling Rate Period and the Asymptotic Temperature of the Moist Part

By

Ryozo TOEI* and Shinya HAYASHI*

(Received August 31, 1963)

Experimental investigations of drying of bed of granular and powdered materials were performed. Drying rate, moisture profile and temperature profile were measured. The asymptotic temperature of the moist part was defined. The mechanism of drying process during the falling rate period has been analysed from consideration of a simultaneous heat and mass transfer. The equation to calculate the second falling rate was suggested.

1. Introduction

Drying process is a simultaneous heat and mass transfer phenomena, depending on the external and internal conditions—the physical and chemical characteristics of the material, such as size, shape, voidance, thermal conductivity and surface properties, etc.

It is, therefore, a difficult problem to analyse the drying mechanism on account of the widely varying physical and chemical characteristics of materials and a perfect theory of drying mechanism has not been presented yet in spite of considerably great efforts.

But it is necessary and requested for a rational design of dryers from a chemical engineering point of view, to predict the drying rate theoretically, based on the drying mechanism, rather than experimentally.

From the point of this view, we have been trying to analyse the drying process as a simultaneous heat and mass transfer phenomenon by measuring the drying rate, temperature- and moisture-profiles at the same time.

We have performed mainly the experiments of convective air drying of a bed of non-porous and non-adsorptive granular and powdered materials (sand, glass beads, plastic beads and powders of various inorganic substanses) at constant conditions of drying air temperature, humidity and air velocity.

* Department of Chemical Engineering

2. Experimental Equipment and Procedure

The outline of the experimental equipment for drying is shown in **Fig. 1.** Air is blown into the equipment by a blower and humidified in the humidificating packed-tower by contacting directly with circulating water cooled by a refrigerator, then heated to a desired temperature at the air heater by electrical heating. The temperature and humidity of air is severely controlled by setting the air temperature and circulating water temperature to constant values, respectively.

The measuring parts of this equipment are set in a wind tunnel with a double wall for reducing the heat loss through the wall. The wind tunnel is made of wood due to its low thermal conductivity.

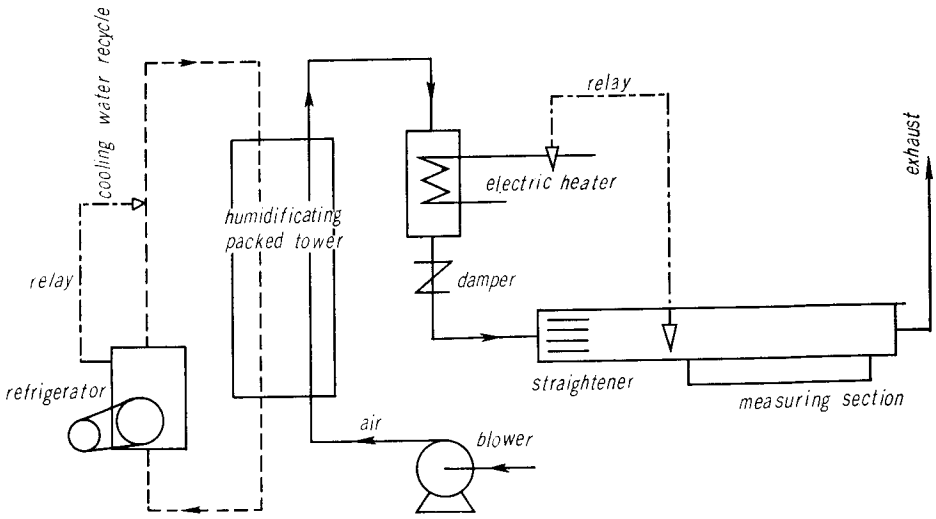

Fig. 1. Shematic diagram of the experimental equipment.

The length of the wind tunnel is 150 cm and its cross section rectangular, 12 cm width and 8 cm height.

Air stream is straightened by a straightener, which ensures uniform distribution of air velocity across the tunnel section. Air velocity is controlled by a damper and is measured by a hot wire anemometer. As shown in Fig. 1, measuring parts are set in this tunnel. These parts consist of three parts A, B, and C, as shown in **Fig. 2.**

The container A is used for measuring the weight change. This is made of $1\frac{1}{2}$ inch polyethylene pipe.

Polyethylene is used for its low thermal conductivity for reducing the heat transfered to the bed through the wall and bottom of the container.

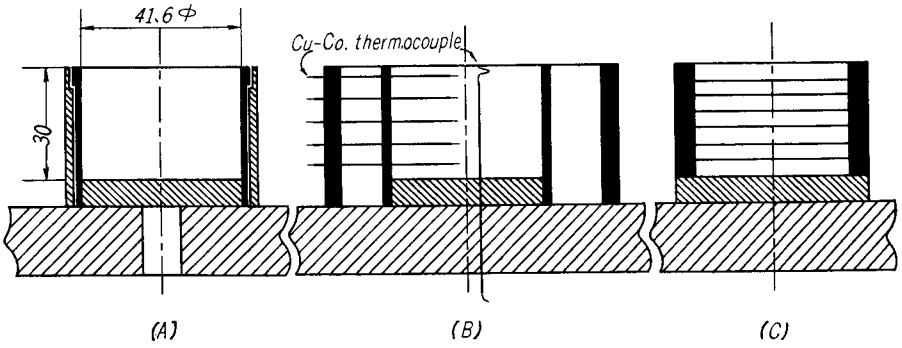

Fig. 2. Details of measuring parts.

At any decided time, this container is taken out and weighed quickly with a direct reading balance (precision of 0.1 mg). The average moisture content is calculated and the drying rate is derived by graphical differentiation of data of change of average moisture contents with time.

The container B is for measurement of temperature distribution. It is made of a double tube of $1\frac{1}{2}$ and $2\frac{1}{2}$ inch polyethylene pipes, and the wet material is packed in the $1\frac{1}{2}''$ tube and in the anular space of the $1\frac{1}{2}''$ and $2\frac{1}{2}''$ tubes.

Six Cupper-Constantan thermocouples are pierced into the container B and connected with a recorder, so that temperature changes at each depth with time is recorded continuously.

Eleven containers C are arranged in a box and are prepared for measurement of moisture distribution. Each container C consists of accumulated polyethlene rings (dia. $1\frac{1}{2}''$) and the depth of this container C is mainly 3 cm and each hight of the ring is ca. 3 mm, hence 9 rings are accumulated and wrapped by tape.

The space between each container C arranged in a box is filled by the same material of the same moisture content to reduce the heat transfered to the container from its wall to a minimum. The bottom of the box is insulated by asbestos and glass-fiber.

At any desired time, one container is taken out and the container is sliced into 9 rings. The moisture content of the material of each ring is determined. The material is packed into the containers carefully to maintain a constant void fraction. The materials used for experiments are given in **Table 1.**

They are mainly non-porous and non-adsorptive granular and powdered materials. The ranges of experimental conditions are given in **Table 2.**

All variables of experiments, such as air conditions, materials, depths of bed and initial moisture contents are changed widely.

Table 1. Characteristics of material used.

Material	Diameter	Density kg/m³	Bulk density kg/m³	Effective thermal conductivity of dried bed kcal/m·hr·°C	Specific heat kcal/kg·°C	Shape of particle
Acricon I [a]	42～ 60#	1100	536	0.058	0.35	sphere
Acricon II	60～ 80#	1100	683	0.075	0.35	〃
Acricon III	150～200#	1190	720	—	0.35	〃
Sand I [b]	28～ 35#	2700	1300	0.110	0.19	
〃	60～ 80#	2700	1300	0.110	0.19	
Sand II [c]	32～ 48#	2520	1500	0.196	0.19	
Sand III	60～ 80#	2550	1140	0.110	0.19	
glass beads I	30～ 50#	2520	1480	0.175	0.23	sphere
〃 II	50～ 90#	2520	1350	0.175	0.23	〃
〃 III	90～120#	2520	1470	0.182	0.23	〃
P.V.C. beads [d]	60～ 80#	1200	485	0.074	0.36	〃
activated alumina beads	20～ 32#	—	714	0.092	0.24	〃
calcium carbonate	0.3～ 2μ	2700	1600	0.108	0.19	
barium sulfate	1～ 2μ	4350	1680	—	—	
titanium oxide	1～ 2μ	3900	1084	—	—	
talc	2～40μ	2700	1265	—	—	
lithopone [e]	1.5～ 2μ	2300	1710	—	—	

a) beads of poly methylmetaacrylate resin
b) crushed sand
c) sand of Kizu river
d) polyvinylchloride resin
e) ZnS 28%, $BaSO_4$ 72%

Table 2. Range of experimental conditions.

air temperature	40～110°C
air humidity	0.004～0.024 kg-H_2O/kg-dry air
air velocity	1～10 m/sec
depth of bed	0.02～0.05 m

3. Experimental Results

3.1. General observation

Drying rate: The forms of the drying rate curves vary with the characteristics of materials, but there are something in common. A typical curve obtained from these experiments is shown in **Fig. 3.** There are three parts AB, BC and CD in this curve. At AB, the rate remains substantially constant down to a critical moisture content—the constant rate period.

BC shows a linear reduction in rate with the water content—first falling rate period.

CD portion is a concave form to upward—second falling rate period.

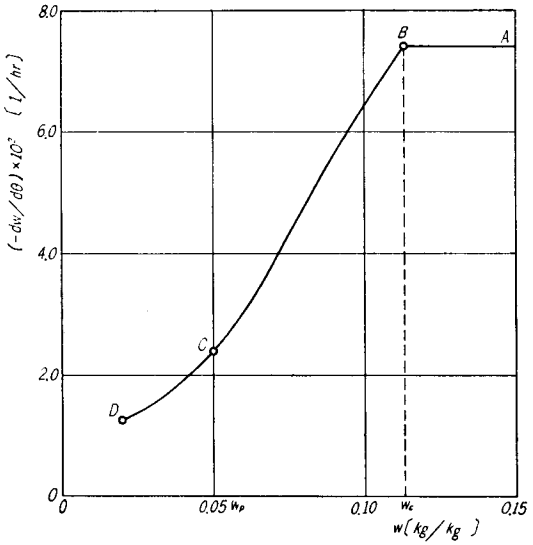

Fig. 3. Typical drying rate curve.
(Run No. 3-90, fine powder of $CaCO_3$, t_a=90°C, H_a=0.0076, V_a=5.58 m/sec, L=0.03 m)

Moisture distribution: The form of moisture distribution curve is complicated and varies with the characteristics of materials also.

But it is observed through several points in common through data. Some typical curves are shown in **Fig. 4.**

(a) At the neighbourhood of the critical moisture content, the form of moisture distribution curve becomes to be nearly parabolic.

(b) Below the critical moisture content, the moisture distribution curves shift retaining their parabolic form.

(c) Surface moisture content reduces and reaches to the equilibrium moisture concentration.

Average moisture content at this time is named the second critical moisture content w_p.

(d) After that, the evaporating plane goes back into the bed, thereby dried-up zone and wetted zone appear in the bed.

Temperature distribution: **Fig. 5** shows time-temperature plots at different depth. During the constant rate period, temperature remains constant nearly

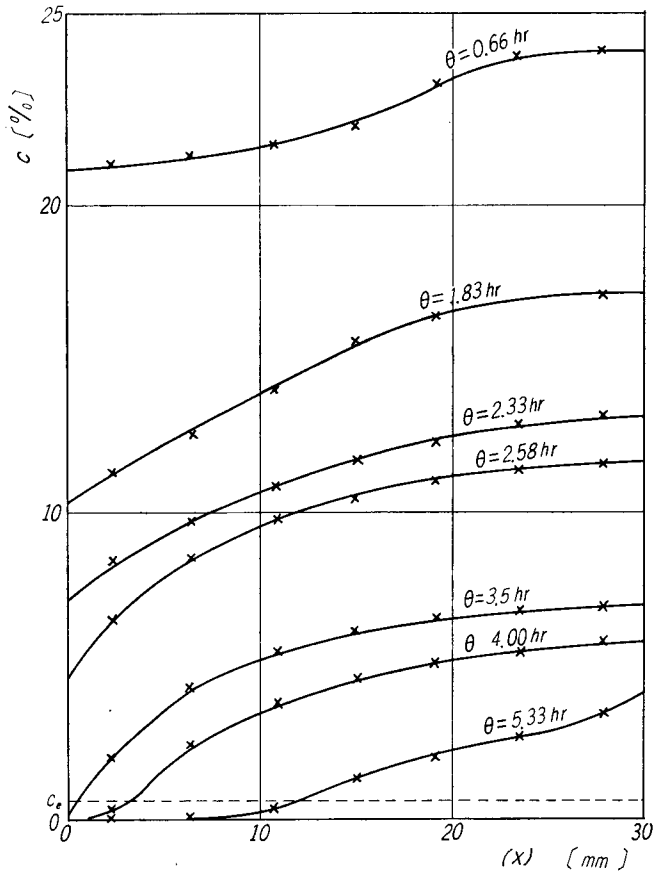

Fig. 4. Moisture distribution curves.
(Run 3-90, fine powder of $CaCO_3$, same experiment shown in Fig. 3)

equal to the wet bulb temperature at each depth.

After the critical moisture content has been reached, temperatures begin to rise as follows.

During the first falling rate period, temperature at each depth rises to a nearly constant temperature. After the second critical moisture content, temperature of the upper portion of bed begins to approach rapidly to air temperature from that temperature. On the other side, temperature of the lower portion remains nearly constant but is on the increase slightly, and then rapidly approaches to the air temperature.

As described before, in the second falling rate period, the bed is separated into a dried-up zone and wetted zone, so it is considered that the zone remaining

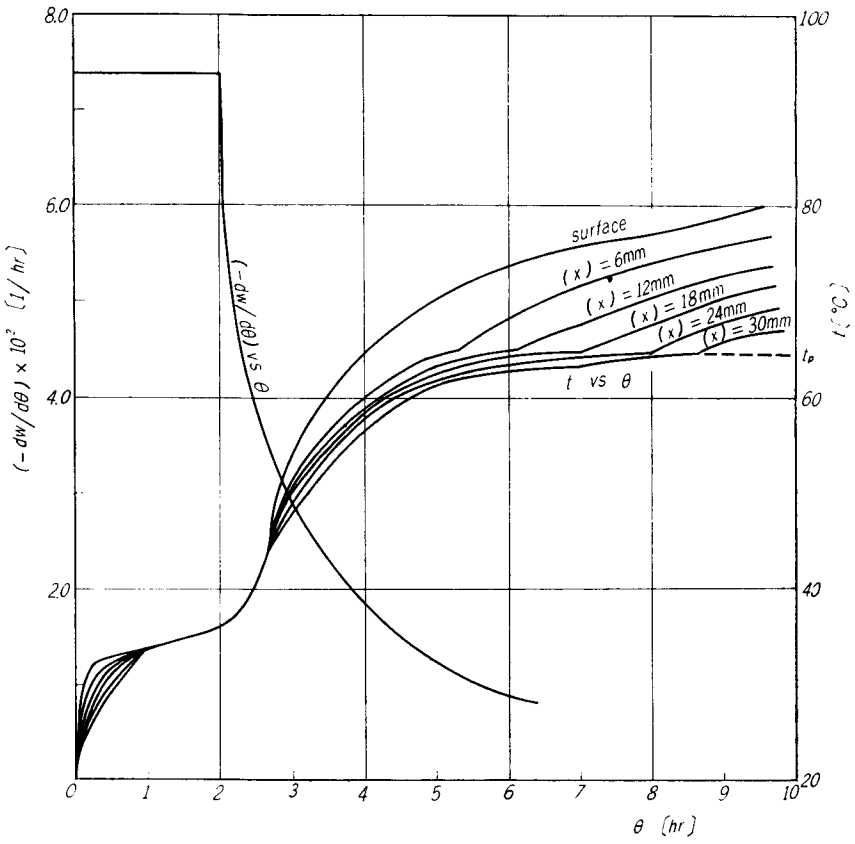

Fig. 5. Temperature cistribution curves.
(Run No. 3-90, fine powder of $CaCO_3$, same experiment shown in Fig. 3)

at nearly constant temperature corresponds to the moist part. This may be discussed in a later section.

Overall observation : Summarizing the drying rate, moisture and temperature distribution curves, the following facts can be observed.

(a) The average moisture content at point C in Fig. 3 which is the break-point of the drying rate curve, is equal to the second critical moisture content, w_p.

(b) Furthermore, the average moisture content at which the surface temperature is equal to the nearly constant temperature described in temperature profile, is also equal to w_p.

3. 2. Drying mechanism of second falling rate period

The mechanism for the first falling rate period is not investigated sufficiently. This may be discussed later in another paper. Thus we will discuss the

mechanism for the second falling rate period in this paper. As mentioned above, as drying proceeds, the surface moisture content reduces and reaches to the equilibrium moisture content.

From this point, the second falling rate period begins.

The evaporating plane retreats into the bed and dried-up zone begins to grow from the surface. As shown in Fig. 5, at the beginning of the second falling rate period temperature is not so different at each depth.

Thereafter, the temperature of the upper portion begins to rise rapidly to air temperature, on the other side, temperature of the lower portion remains nearly constant but is on the increase slightly.

These two characteristics of temperature rising are quite different and will result in moisture distribution. So we will compare the temperature distribution curves with moisture distribution ones.

Another example of temperature and moisture distribution curves on the drying of granular resins of Acricon is shown in **Fig. 6 (a), (b).**

As shown in Fig. 6 (a), x is taken as a distance from surface to a point at

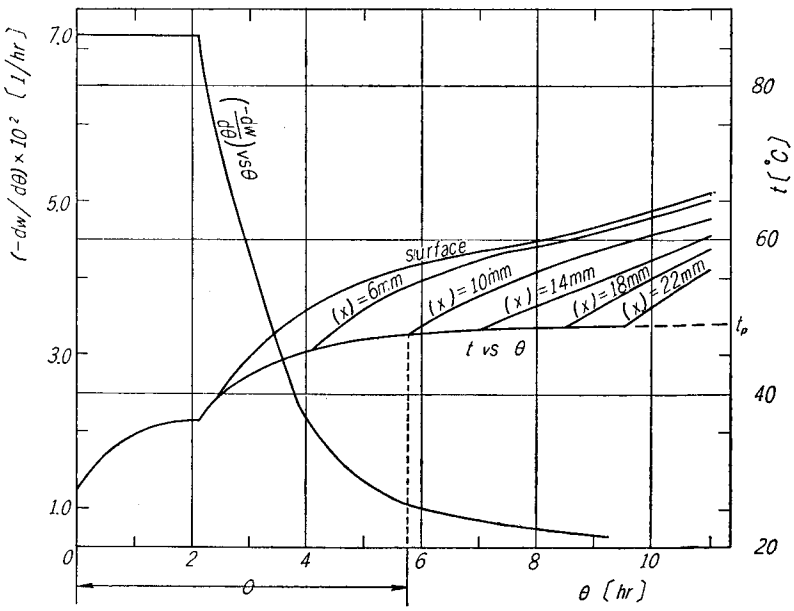

Fig. 6 (a). Temperature distribution curves.
(Run No. Ac-7, Acricon (42~60#) t_a=71.0°C, H_a=0.0113, V_a=1.8 m/sec, L=0.03 m)

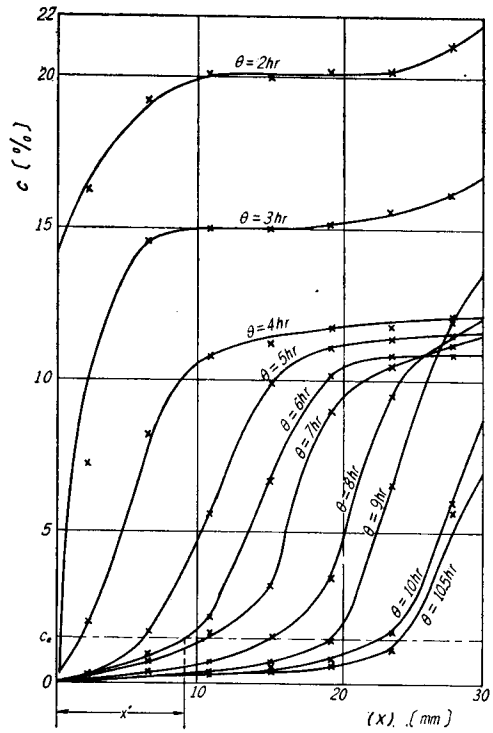

Fig. 6 (b). Moisture distribution curves. (Run No. Ac-7)

which the temperature begins again to approach to air temperature from nearly constant temperature at time θ.

On the one side, as shown in Fig. 6 (b), x' is taken as a distance from surface to point, at which the moisture content becomes the equilibrium moisture content on moisture distribution curve at time θ.

About the experiment of Fig. 6, x and x' are plotted with θ on **Fig. 7** and also plotted about the experiment shown in Figs. 4 and 5.

These two lines of each experiment agree within the range of the experimental error.

So it is deduced that temperature of wetted zone remains at nearly constant but is on the increase slightly and as the evaporating plane goes back, the temperature of dried-up zone approaches rapidly to the air temperature.

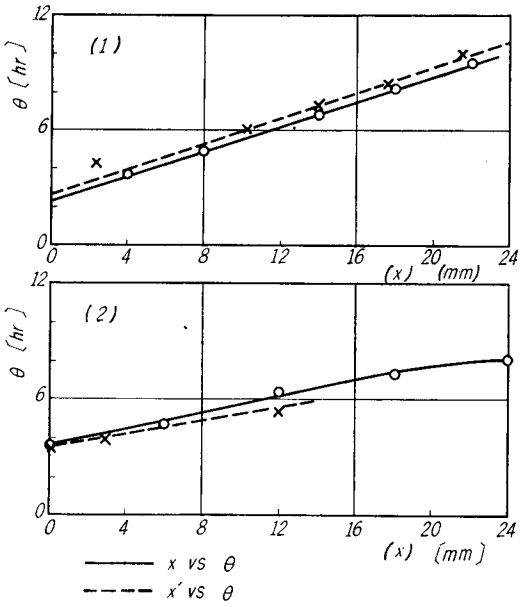

Fig. 7. Comparison between two relations of x and x' vs. θ.
(1) Run No. Ac-7 (2) Run No. 3-90

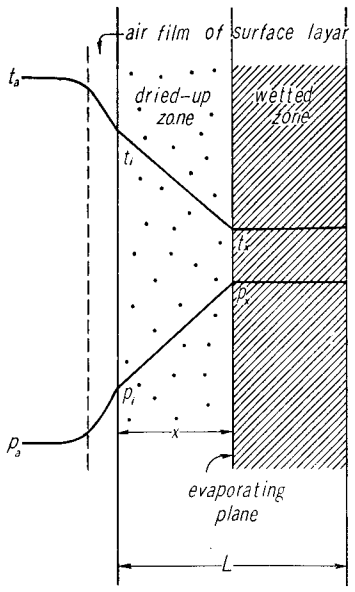

Fig. 8. Shematic model of evaporating surface of bed during the second falling rate period.

4. Theoretical Consideration of a Temperature of Evaporating Plane and an Asymptotic Temperature of the Moist Part

On the basis of the above investigation, the following model is considered for drying process in this period as shown in **Fig. 8.**

The bed is separated into two zones, dried-up zone and wetted zone, and evaporation takes place at the boundary plane between two zones and evaporated vapor reaches to the surface by vapor diffusion through the dried-up zone.

The heat transfered from air to bed at the surface air film is:

$$q = h_t(t_a - t_i)A \qquad (1)$$

and the heat transfered at the dried-up zone is:

$$q = \frac{k_e}{x}A(t_i - t_x) + mc_p\frac{dt}{d\theta} \tag{2}$$

The second term of eq. (2) represents sensible heat for material heating. This is negligibly small compared with the first term within a few percent. From eq. (1) and (2):

$$q = \frac{A(t_a - t_x)}{\frac{1}{h_t} + \frac{x}{k_e}} \tag{3}$$

Considering the mass transfer at the surface air film:

$$q = k'(p_i - p_a)/R_w T_{av} \tag{4}$$

at the dried-up zone:

$$G = \frac{D}{\mu x}(p_x - p_i)/R_w T_{av} \tag{5}$$

From eqs. (4) and (5):

$$G = \frac{(p_x - p_a)}{\left(\frac{1}{k'} + \frac{\mu x}{D}\right)R_w T_{av}} \tag{6}$$

Combining heat and mass transfer,

$$G = q/r_x \tag{7}$$

Thereby we obtain eq. (8) from eqs. (3), (6) and (7):

$$\frac{(t_a - t_x)}{\left(\frac{1}{h_t} + \frac{x}{k_e}\right)r_x} = \frac{(p_x - p_a)}{\left(\frac{1}{k'} + \frac{\mu x}{D}\right)R_w T_{av}} \tag{8}$$

Eq. (8) is considered to represent the temperature of evaporating plane t_x. At eq. (8), p_x is determined from water vapor pressure at temperature t_x.

When x becomes to be sufficiently large, we can put $x/k_e \gg 1/h_t$ and $\mu x/D \gg 1/k'$ in eq. (8) and write t_x as t_p in this case, hence eq. (8) becomes,

$$\frac{(t_a - t_p)}{(p_p - p_a)} = \frac{r_p D}{k_e \mu R_w T_{av}} \tag{9}$$

The temperature t_p is defined as an asymptotic temperature of t_x when x approches to infinity.

The temperature of evaporating plane t_x has an asymptotic value of t_p and this t_p can be calculated from the transport properties of bed and air conditions by eq. (9). The effective thermal conductivity of the dried bed, k_e, was measured experimentally by a non-steady heating method of cylindrical packed bed.[1] The diffusion coefficient of water vapor in the air can be calculated.[2] For the

resistance coefficient of diffusion μ, experimental data are poor. Krischer[3] has made precise researches about μ and concluded that $\mu=\mu_1/\varepsilon$ and for random packing of spheres $\mu_1=1.57$ and Nissan[4] stated that $\mu=1/\varepsilon$. Calculation of μ was performed using the values suggested by Krischer and Nissan in our case. Using these values, t_p can be calculated.

Experimental and calculated values are shown on **Table 3.**

Table 3. Comparison between experimental and calculated values of t_p.

Material	$CaCO_3$	$CaCO_3$	$CaCO_3$	$CaCO_3$	Sand I	Sand I
t_a (°C)	50	70	70	90	50	70
p_a (Kg/m²)	143.5	125.5	125.5	125.5	125.5	125.5
ε	0.472	0.460	0.467	0.451	0.523	0.498
k_e	0.108	0.108	0.108	0.108	0.110	0.110
$t_{p\,exp}$ (°C)	42.7	55.7	56.0	64.5	39.7	51.8
$t_{p\,cal_1}$ (°C)	40.0	50.6	50.7	59.5	39.5	52.5
$t_{p\,cal_2}$ (°C)	(43.0)	(54.4)	(54.5)	(64.4)	(41.6)	(54.0)

Material	Sand I	Acricon I	Acricon I	Acricon II	P.V.C.	Glass beads II
t_a (°C)	95	70	70	70	77	73.0
p_a (Kg/m²)	125.5	189.5	189.5	186.5	148.5	128.0
ε	0.553	0.465	0.501	0.481	0.596	0.460
k_e	0.110	0.058	0.058	0.075	0.074	0.175
$t_{p\,exp}$ (°C)	60.4	47.0	49.5	50.0	46.5	53.7
$t_{p\,cal_1}$ (°C)	59.0	45.5	45.0	47.7	47.0	57.0
$t_{p\,cal_2}$ (°C)	(65.1)	49.8	49.3	51.3	52.1	60.2

Material	Glass beads III	Glass beads III	Glass beads I	Glass beads I
t_a (°C)	71.2	50.6	50.4	71.3
p_a (Kg/m²)	170.0	158.5	160.0	158.5
ε	0.474	0.474	0.470	0.420
k_e	0.182	0.182	0.175	0.175
$t_{p\,exp}$ (°C)	54.0	43.0	42.5	54.3
$t_{p\,cal_1}$ (°C)	55.5	43.0	42.7	56.3
$t_{p\,cal_2}$ (°C)	59.2	45.1	44.8	59.6

Note : 1. $t_{p\,cal_1}$ is calculated by $\mu=1/\varepsilon$
$t_{p\,cal_2}$ is calculated by $\mu=1.57/\varepsilon$
2. Values of $t_{p\,cal_2}$ for materials of non-spherical particles (Sand and $CaCO_3$) are shown for reference.

The calculated values agree approximately with the experimental ones.

We have calculated also the values of μ from eq. (9) by using the experimental values of t_p. The results are shown in **Table 4.**

Values of μ_{exp} are more closed to μ_{cal_2} for Acricon, $CaCO_3$ and sand than

μ_{cal_1}, but values of μ_{exp} for glass beads and P.V.C. are closed to μ_{cal_1} rather than μ_{cal_2}.

A little heat loss through bottom of containers might be considered in our experiments and true values of t_p and so μ might show some higher ones than $t_{p\,exp}$ and μ_{exp} when a heat loss is completely vanished.

Nissan[4,5,6] has stated that the temperature t_x is constant and has named it as "pseudo wet-bulb temperature", but as shown in eq. (8) t_x should vary with x and this value has an asymptotic value of t_p.

Table 4. Comparison between experimental and calculated values of μ.

Material	Acricon I	Acricon I	Acricon II	$CaCO_3$	$CaCO_3$	$CaCO_3$	$CaCO_3$
t_a (°C)	70	70	70	50	70	70	90
p_a (Kg/m²)	189.5	189.5	186.5	143.5	125.5	125.5	125.5
$t_{p\,exp}$ (°C)	47.0	49.5	50.0	42.7	55.7	56.0	64.5
μ_{exp}	2.76	3.40	2.90	4.44	4.44	4.52	3.45
$\mu_{cal_1}=1/\varepsilon$	2.15	2.0	2.08	2.11	2.18	2.13	2.22
$\mu_{cal_2}=1.57/\varepsilon$	3.37	3.14	3.26	(3.30)	(3.42)	(3.34)	(3.49)

Material	Sand I	Sand I	Sand I	Glass beads III	Glass beads I	P.V.C.
t_a (°C)	50	70	95	71.2	50.4	77
p_a (Kg/m²)	125.5	125.5	125.5	170.0	160.0	148.5
$t_{p\,exp}$ (°C)	39.7	51.8	60.4	54.0	42.5	46.5
μ_{exp}	2.69	2.76	2.10	1.82	2.09	1.74
$\mu_{cal_1}=1/\varepsilon$	1.91	2.01	1.81	2.11	2.13	1.68
$\mu_{cal_2}=1.57/\varepsilon$	(3.0)	(3.16)	(2.84)	3.30	3.34	2.63

Note : Values of μ_{cal_2} for materials of non-spherical particles (Sand and $CaCO_3$) are shown for reference.

5. Drying Rate Expression in Second Falling Rate Period

About the drying rate of this period, the following rate expression can be obtained. If the sensible heat of material heating is negligible, eq. (3) can be rewritten to the drying rate expression,

$$-\frac{dw}{d\theta}=\frac{1}{\rho' L r_x}\frac{(t_a-t_x)}{\dfrac{1}{h_t}+\dfrac{x}{k_e}} \tag{10}$$

Except the region that x is very small, we can put approximately $t_x=t_p$. The difference of t_x at 6 mm depth and t_p is only 1~3°C by our experiments.

And h_t is replaced by h_p which is the heat transfer coefficient at $w=w_p$. Then eq. (10) becomes :

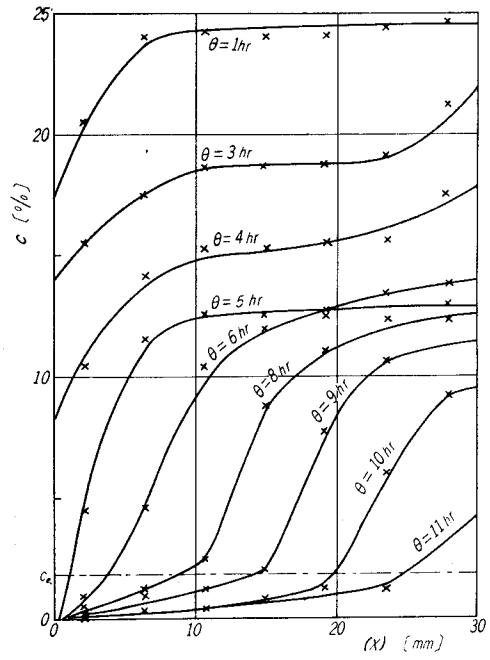

(a)

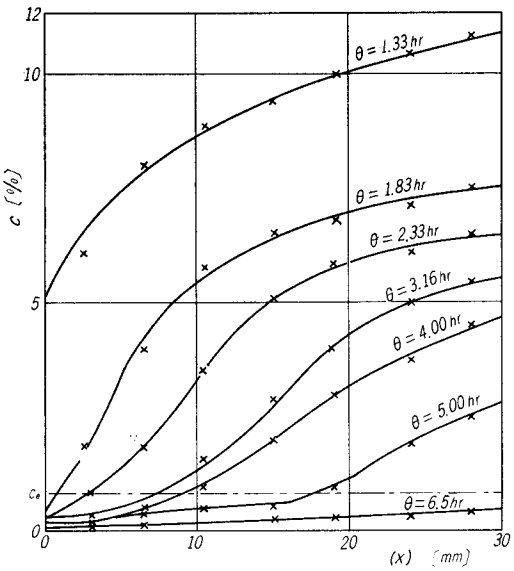

(b)

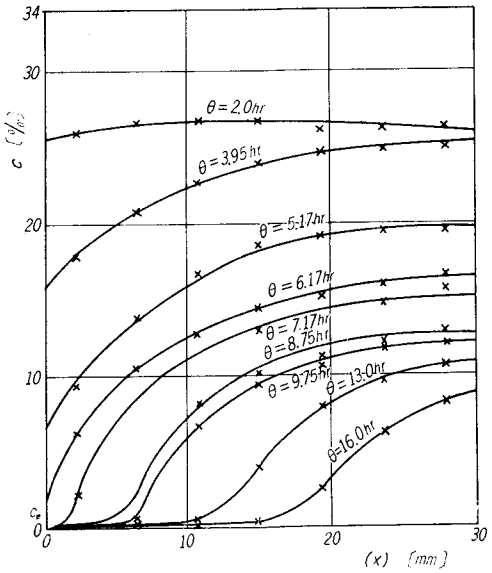

(c)

Fig. 9. Moisture distribution curves.
(a) (Run No. Ac-9, Acricon (60~80#),
t_a=70°C, H_a=0.0112, V_a=1.7 m/sec, L=0.03 m)
(b) (Run No. S-3-95, Sand I (28~35#),
t_a=95°C, H_a=0.0076, V_a=5.63 m/sec, L=0.03 m)
(c) (Run No. T-1, talc,
t_a=87.1°C, H_a=0.0058, V_a=2.9 m/sec, L=0.03 m)

$$-\frac{dw}{d\theta}=\frac{1}{\rho' L r_p}\frac{(t_a-t_p)}{\frac{1}{h_p}+\frac{x}{k_e}} \tag{11}$$

We must represent x by term of w or θ to transform eq. (11) to a convenient expression. From experimental moisture distributiots, x can be expressed as a function of w.

It is observed from the experimental moisture distribution curves during the second falling rate period that the evaporating surface retreats into the bed keeping a simple geometric pattern of moisture distribution as shown in **Fig. 9.** (a) (b) (c).

The moisture distributions in the second falling rate period are classified in three types as shown in Figs. 9 (a), (b) and (c).

As shown in Fig. 6 (b) and Fig. 9 (a), the evaporating plane retreats into the bed stepwisely and this is found on the drying of Acricon and activated alumina. On Fig. 9 (b), it retreats into the bed as the parallel shifting of straight lines and this is found on sand layer drying.

On Fig. 4 and Fig. 9 (c), it retreats into the bed as the parallel shifting of parabolas and this is found on the drying of glass beads and fine powders of synthetic resin of P. V. C., calcium carbonate and other inorganic substances (lithopone, titanium oxide, barium sulphate and talc).

From these figures, the models of moisture distributions can be drawn as **Fig. 10 (a) (b) (c).**

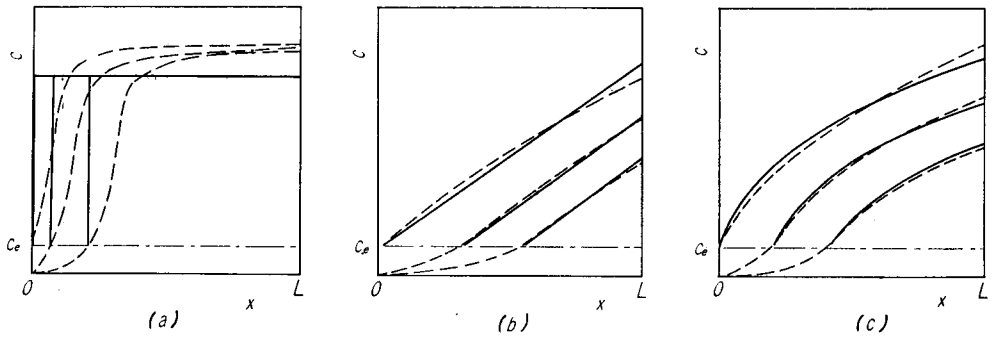

Fig. 10. Shematic models of moisture distribution curves during the second falling rate period.

In these models, the following relation between x and w can be obtained geometrically,

$$\frac{x}{L}=1-\left(\frac{w}{w_p}\right)^{1/n} \tag{12}$$

In cases of Fig. 10 (a), (b) and (c), the value of n is 1, 2 and 3 respectively. That is, at (a) $n=1$, at (b) $n=2$ and at (c) $n=3$.

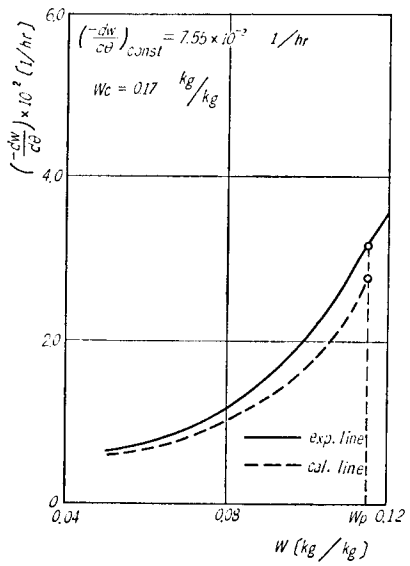

(a)

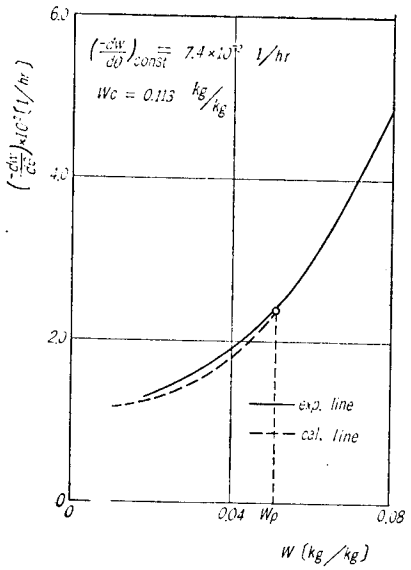

(b)

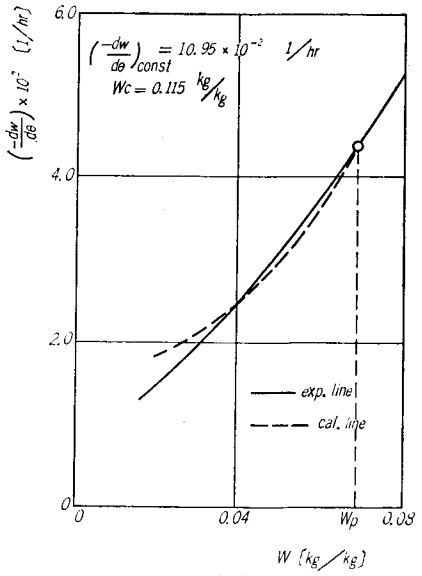

(c)

Fig. 11. Comparison between experimental and calculated drying rate.
(a) (Run No. Ac-7, same experiment shown in Fig. 6)
(b) (Run No. S-3-95, same experiment shown in Fig. 9(b))
(c) (Run No. 3-90, same experiment shown in Figs. 3~5)

Replacing the relation of eq. (12) into eq. (11), we can obtain the final expression of second falling rate:

$$-\frac{dw}{d\theta}=\frac{1}{\rho' L r_p}\frac{(t_a-t_p)}{\frac{1}{h_p}+\frac{L}{k_e}\left(1-\left(\frac{w}{w_p}\right)^{1/n}\right)} \tag{13}$$

The calculated values of drying rate from eq. (13) are shown in **Fig. 11** (**a**), (**b**), (**c**) with the experimental values. It is observed that the calculated values agree sufficiently with the experimental ones.

So eq. (13) can be used as the drying rate equation during the second falling rate period.

Bates[7] mentioned that the evaporating plane retreats into the bed stepwisely, and the temperature of the evaporating plane is the wet-bulb temperature of the surrounding air. But by our experiments, the temperature of the evaporating plane is not the wet-bulb temperature but t_x and there are three types of moisture distribution as shown on Fig. 9 and 10.

6. Conclusion

From our experiments of moisture and temperature profile, the following facts are investigated:

(1) Drying period are distinguished to three periods, i. e. constant rate period, first and second falling rate periods.

(2) At the second critical moisture content w_p, the surface moisture content reaches to an equilibrium moisture coutent, then evaporating surface retreats into the interior of the bed.

(3) The temperature of this evaporating plane remains nearly constant and approaches to an asymptotic temperature t_p defined by eq. (9).

(4) The value of t_p can be calculated from the transport properties of bed and air conditions by eq. (9).

(5) Moisture distributions during the second falling rate period are classified in three types as shown on Fig. 10 (a), (b), (c).

(6) The drying rate during the second falling rate period can be calculated by eq. (13).

Acknowledgment

The authors wish to express their appreciations to Professor Dr.-Ing. O. Krischer for his kind suggestions to this work.

Nomenclature

A	:	area	[m^2]
c	:	local moisture content	[%]
c_e	:	equlibrium moisture content	[%]
c_p	:	specific heat of material	[kcal/kg·°C]
G	:	rate of flow of water vapor	[kg/hr]
H	:	humidity of air	[kg/kg-dry air]
h_t	:	overall heat transfer coefficient	[kcal/m^2·hr·°C]
k'	:	mass transfer coefficient	[m/hr]
k_e	:	effective thermal conductivity of dried bed	[kcal/m·hr·°C]
L	:	depth of bed	[m]
m	:	mass of bed material	[kg]
p	:	partial pressure of water vapor	[Kg/m^2]
q	:	rate of flow of heat	[kcal/hr]
r	:	latent heat of evaporation of water	[kcal/kg]
R_w	:	gas constant of water vapor	[47.1 Kg·m/°K·kg]
t	:	temperature	[°C]
t_p	:	asymptotic temperature of moist part	[°C]
V_a	:	velocity of hot air	[m/sec]
w	:	average moisture content	[kg/kg]
w_c	:	critical moisture content	[kg/kg]
x	:	distance from surface	[m]
ε	:	porosity	[−]
μ	:	resistance coefficient for vapor diffusion through bed	[−]
ρ'	:	bulk density of dried bed	[kg/m^3]
θ	:	time	[hr]

Suffix

a : air
i : interface
p : value at w_p
x : value at distance x

Literature

1) Kimura, M.: Chem. Eng. (Japan), **21,** 472 (1957), **23,** 502 (1959)
2) Gilliland, E. R.: Ind. Eng. Chem., **26,** 681 (1934)
Schrimer, R.: Z. VDI., **6,** 524 (1938)
3) Krischer, O.: "Die wissenschaflichten Grundlagen der Trocknungstechnik". Bd. I 2 Aufl. s. 212 (1963)
4) Nissan, A. H.: George, H. H., Jr. and Bolles, T. V.: A. I. Ch. E. J., **6,** 406 (1960)
5) Nissan, A. H., Kaye, W. G. and Bell, J. R.: ibid **5,** 103 (1959)
6) Nissan, A. H. and Bell, J. R.: ibid 344 (1959)
7) Bates, H. F.: Chem. Eng. Prog., **56,** 52 No. 11 (1960)